New Barium Rare-Earth Nickel Oxides: Synthesis, Crystal Structure, and Magnetic Order

ARTICLE *in* CHEMISTRY OF MATERIALS · NOVEMBER 1998

Impact Factor: 8.35 · DOI: 10.1021/cm980126j

New Barium Rare-Earth Nickel Oxides: Synthesis, Crystal Structure, and Magnetic Order

E. Gutiérrez-Puebla,† M. A.Monge,*,† C. Ruiz-Valero,† and J. A. Campá‡

Instituto de Ciencia de Materiales de Madrid, CSIC, Cantoblanco, 28049 Madrid, and Facultad de Ciencias Geológicas, Universidad Complutense 28040 Madrid, Spain

Received March 3, 1998. Revised Manuscript Received July 6, 1998

Crystals of isostructural $R_8Ba_5Ni_4O_{21}$ (R = Y, Er, Tm, Yb, and Lu) have been obtained. Conditions for synthesis and stability are reported. The crystal structures of these materials have been established by single-crystal X-ray diffraction: space group *I*4/*m* with cell-parameters a =13.713(1) and 13.666(3) Å, c = 5.692(1) and 5.673(2) Å for R = Y and Er, respectively. The compounds contain square NiO_5 pyramids, trigonal RO_7 prisms capped on one rectangular face, tetragonal bicapped $Ba(1)O_{10}$ prisms, and irregular $Ba(2)O_{10}$ polyhedra. A comparison is made between this structure type and those of R_2BaNiO_5 and R_2BaCuO_5. Their structure and properties show close relations. The temperature dependence of the magnetic susceptibility from 350 to 1.8 K, measured for R = Y, Yb, and Er, shows the presence of antiferromagnetic ordering for the Yb and Er compounds.

Introduction

Phase equilibria in ternary and higher-order Ni oxide systems have been subject of intense investigation over the past few years as a consequence of the interest in the green-colored oxides R_2BaNiO_5.[1] The existence of several phases in the system Ba−Ni−O was reported by Lander[2,3] and Takeda.[4] Recently, higher oxides of nickel with Ba/Ni > 1, such as $BaNi_{0.83}O_{2.5}$,[5] belonging to the perovskite-related $A_{3n+3}A'_nB_{3+n}O_{9+6n}$ family[6,7] (*A* = alkaline-earth metal), are being studied.

In the Y−Ba−Ni−O system in air between 1000 and 1300 °C, the existence of an unknown Ba-rich phase has been suggested,[8] in addition to a good number of the mentioned binary oxides, the R_2BaNiO_5 compound, and two more well-defined R−Ba−O phases. In a previous work, we reported a new family of compound $R_8Ba_5Ni_4O_{21}$ for the three smallest lanthanides (R = Tm, Yb, and Lu),[9] establishing its structural type. Afterward, other oxometalates of manganese (II) of generic formulas $Ba_5Mn_4R_8O_{21}$, which belong to this same structural type, have been reported.[10,11] Because interesting relations can be found between crystal structure and magnetic properties of these oxometalates containing **d** and **f** cations, the authors tried to grow crystals of those oxides of this family formed by larger lanthanides. The aims of this work are to investigate the variation of the structural type as a function of the rare-earth ionic size, to study the existence of magnetic interactions among the mentioned cations, and to situate the $R_8Ba_5Ni_4O_{21}$ family in the R−Ba−Ni−O phase diagram. Here, the results of attempts to synthesize compounds with Y, Sm, Er, Ho, and La, the crystal structure for Y and Er, and the result of magnetic measurements from 350 to 1.8 K for compounds with R = Y, Yb, and Er are reported.

Experimental Section

Crystal Growth and Sample Preparation. Because of the high melting point of the $R_8Ba_5Ni_4O_{21}$ series compounds and to the difficulty of obtaining single crystals free of flux contamination, we followed a two-step synthesis path based on the exothermic solid-state reaction between $BaCO_3$ (AR) and Ni (99.95%) metal at 1300 °C, that gives a liquid precursor $BaNiO_{2+x}$. In a second step, the precursor reacts with a mixture of R_2O_3 (99.9%) and $BaCO_3$ in a ratio R:Ba = 4:1. Final products are obtained by heating this mixture in air for 3 days at 1300 °C. After removing the flux with acetic acid, paper filtration allowed recovery of the crystals that were characterized by energy-dispersive X-ray analysis and X-ray powder diffraction.

After several unsuccessful attempts to synthesize these compounds in microcrystalline form (reactions always yield the R_2BaNiO_5 phase, regardless of the stoichiometric proportions or the synthesis route), samples for magnetic measurements were prepared by powdering well-characterized single crystals. Routine X-ray powder diffraction patterns showed single-phase samples and quite similar parameters to those obtained from

* To whom correspondence should be addressed. E-mail: nines@immrx1.icmm.csic.es. Telephone: (34)-9-3349025. Fax: (34)-9-3720623.
† Instituto de Ciencia de Materiales de Madrid.
‡ Facultad de Ciencia Geologicas.

(1) Amador, J.; Gutiérrez-Puebla, E.; Monge, M. A.; Rasines, I.; Campá, J. A.; Gómez de Salazar, J. M.; Ruiz-Valero, C. *Solid State Ionics* **1989**, *32/33*, 123.
(2) Lander, J. J. *J. Am. Chem. Soc.* **1951**, *73*, 2450.
(3) Lander, J. J. *Acta Crystallogr.* **1951**, *4*, 148.
(4) Takeda, Y.; Kanamaru, F.; Shimada, M.; Koizumi, M. *Acta Crystallogr.* **1976**, *B32*, 2464.
(5) Campá, J. A.; Gutiérrez-Puebla, E.; Monge, M. A.; Rasines, I.; Ruiz-Valero, C. *J. Solid State Chem.* **1994**, *108*, 230.
(6) Strunk, M.; Müller-Buschbaum, H. K. *J. Alloys Compd.* **1994**, *209*, 189.
(7) Campá, J. A.; Gutiérrez-Puebla, E.; Monge, M. A.; Rasines, I.; Ruiz-Valero, C. *J. Solid State Chem.* **1996**, *126*, 27.
(8) Buttrey, D. J.; Sullivan, J. D.; Rheingold, A. L. *J. Solid State Chem.* **1990**, *88*, 291.
(9) Campá, J. A.; Gutiérrez-Puebla, E.; Monge, M. A.; Rasines, I.; Ruiz-Valero, C. *J. Solid State Chem.* **1991**, *95*, 360.
(10) Klüver, E.; Peters, E.; Müller-Buschbaum, H. K. *J. Alloys Compd.* **1992**, *189*, 101.
(11) Müller-Buschbaum, H. K.; Klüver, E. **1992**, *612*, 21.

10.1021/cm980126j CCC: $15.00
Published on Web 10/09/1998

Table 1. Crystal Data and Structure Refinement for $R_8Ba_5Ni_4O_{21}$ (R = Y and Er)

parameter	R = Y	R = Er
empirical formula	$Y_8\ Ba_5Ni_4O_{21}$	$Er_8\ Ba_5Ni_4O_{21}$
formula weight	1968.67	2595.62
temperature	298(2) K	298(2) K
wavelength	0.71073 Å	0.71073 Å
crystal system	tetragonal	tetragonal
space group	*I*4/*m*	*I*4/*m*
unit cell dimensions	a = 13.713(1) Å	a = 13.666(3) Å
	c = 5.6923(8) Å	c = 5.673(2) Å
volume, Z	1070.4(2) Å^3, 2	1059.4(5) Å^3, 2
density (calculated)	6.109 g/cm^3	8.137 g/cm^3
absorption coefficient	33.935 mm^{-1}	43.953 mm^{-1}
F(000)	1744	2208
crystal size	0.10 × 0.10 × 0.10 mm	0.16 × 0.05 × 0.05 mm
Θ range for data collection	2.10 to 23.25°	3.89 to 28.23°
limiting indices	(−14, −15, −5) (15, 13, 6)	(−10, −18, −7) (17, 3, 7)
crystal-detector distance	6.01 cm	5.03 cm
independent reflections	433 (R_{int} = 0.0466)	285 (R_{int} = 0.0109)
absorption correction	semiempirical from psi scans	semiempirical from psi scans
max and min transmission	0.3339 and 0.1486	0.2680 and 0.2293
refinement method	full-matrix least-squares on F^2	full-matrix least-squares on F^2
data/restraints/parameter	433/0/53	285/0/39
goodness-of-fit on F^2	1.097	1.083
final R indices [$I > 2\sigma$ (I)]	R1 = 0.0263, wR2 = 0.0569	R1 = 0.0490, wR2 = 0.1468
R indices (all data)	R1 = 0.0280, wR2 = 0.0577	R1 = 0.0511, wR2 = 0.1491
largest diff peak and hole	0.759 and −1.270 eÅ^{-3}	2.389 and −2.936 eÅ^{-3}

single crystal: a = 13.715(1), 13.668(1), and 13.553(2) Å, c = 5.6930(9), 5.6792(9), and 5.641(1) Å for Y, Er, and Yb, respectively

X-ray Structure Determination. Black crystals (R = Y, Er, Sm−Ho, and La) showing well-defined faces were mounted on a Siemens Smart CCD (charge couple device) diffractometer equipped with MoKα radiation. Data were collected over a hemisphere of the reciprocal space by a combination of three exposure sets for the Y compound, and over a quadrant with two sets for the Er one. Each exposure of 20 s covered 0.3° in ω. Unit cell dimensions were determined by a least-squares fit of 60 reflections and with I>20σ(I). A summary of the fundamental crystal and refinement data for R = Er and Y is given in Table 1. Single crystals of Sm, Nd, Gd, and Ho compounds were identified in the X-ray preliminary study as R_2BaNiO_5, and the one of La as La_2NiO_4, thus their data collection were not performed.

Most of the calculations were carried out with SMART software for data collection[12] and data reduction, and Shelxtl.[13]

Magnetic Measurements. Direct current (dc) magnetic measurements were carried out using a SQUID (Quantum Design) magnetometer operating from 350 to 1.8 K at 1000 Oe.

Results and Discussion

Applying the crystal growth procedure explained in the Experimental Section, different results were obtained depending on the lanthanide involved in the reaction. X-ray single-crystal procedures showed that when La is involved, the obtained compound is always $La_{2-x}Ba_xNiO_4$ with the K_2NiF_4 structure type, in which La and Ba are sharing the same position in a disordered way.[14] For Sm, Nd, Gd, and Ho, only the well-known orthorhombic *Immm* R_2BaNiO_5[15] oxides were formed.

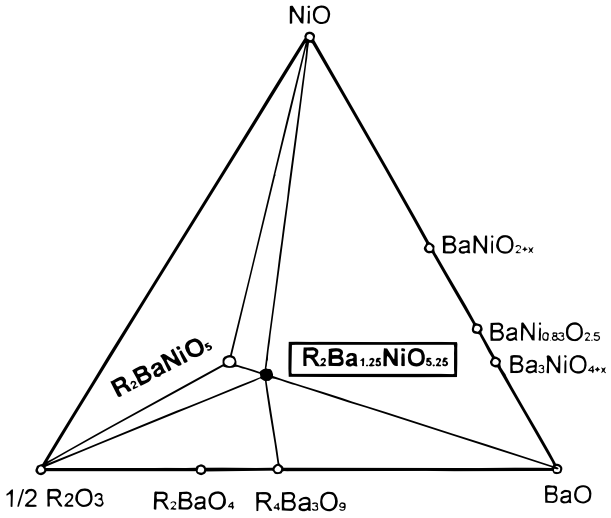

Figure 1. The R−Ba−Ni−O phase diagram in air in the temperature range 1000−1350 °C, showing the Ba-rich $R_8Ba_5Ni_4O_{21}$ phase, named as $R_2Ba_{1.25}NiO_{5.25}$ with comparative purposes.

The tetragonal *I*4/*m* $R_8Ba_5Ni_4O_{21}$ family has only been obtained for R = Y, Er, Tm, Yb, and Lu.

Although by this synthesis procedure each phase is obtained separately, the first time we noticed the existence of this new composition was serendipitously trying to grow crystals of the R_2BaNiO_5 oxides. This fact, together with the temperature range in which this family appears, indicates that the unknown Ba-rich phase whose existence has been suggested in the literature for the R−Ba−Ni−O system, is $R_8Ba_5Ni_4O_{21}$. Figure 1 shows the position of this new family in the named diagram.

$R_8Ba_5Ni_4O_{21}$ crystals are always black and show forms of very faceted prisms elongated along the c axis with maximum length of 4 mm. Figure 2 shows the nearly circular section of the crystal as a consequence of the extremely faceted shape of the prisms. Crystallographic data for R = Tm, Yb, and Lu were given in a previous work,[9] and Tables 2 and 3 include the atomic

(12) Siemens. *Data Collection and Procedure. Software for the SMART System*. Siemens Analytical X-ray Instruments Inc., WI, 1995.
(13) SHELXTL Version. 5.05, AXS Siemens, 1996.
(14) Alonso, J. A.; Amador, J.; Gutiérrez-Puebla, E.; Monge, M. A.; Rasines, I.; Ruiz-Valero, C. *Solid State Comm*. **1990**, *76*, *No. 12*, 1327.
(15) Amador, J.; Gutiérrez-Puebla, E.; Monge, M. A.; Rasines, I.; Ruiz-Valero, C.; Fernández, F.; Sáez-Puche, C.; Campá, J. A. *Phys. Rev*. **1990**, *42*, *No. 13*, 7918.

Figure 2. Crystals of $Er_8Ba_5Ni_4O_{21}$, showing the extremely faceted shape of the prisms.

Table 2. Atomic Coordinates (× 10^4) and Equivalent Isotropic Displacement Parameters (Å × 10^3) for $R_8Ba_5Ni_4O_{21}$, (R = Y and Er)

atom		*x*	*y*	*z*	*U*(eq)[a]
Ba(1)	8*h*	5372(2)	1379(1)	0	8(1)
Ba(2)	2*a*	0	0	0	8(1)
R = Y(1)	8*h*	8340(1)	2502(1)	0	5(1)
R = Y(2)	8*h*	4120(1)	3564(1)	0	5(1)
Ni(1)	8*h*	4592(1)	2544(1)	−5000	6(1)
O(1)	2*h*	5000	5000	0	13(4)
O(2)	8*h*	5363(6)	1302(6)	−5000	11(2)
O(3)	16*i*	7405(6)	1461(4)	244(1)	8(1)
O(4)	16*i*	8209(4)	−465(4)	248(1)	9(1)
Ba(1)	8*h*	5376(2)	1383(2)	0	5(1)
Ba(2)	2*a*	0	0	0	5(1)
R = Er(1)	8*h*	8337(1)	2502(1)	0	3(1)
R = Er(2)	8*h*	4118(1)	3566(1)	0	3(1)
Ni(1)	8*h*	4592(1)	2546(4)	−5000	3(1)
O(1)	2*h*	5000	5000	0	7(11)
O(2)	8*h*	537(2)	130(2)	−5000	7(6)
O(3)	16*i*	741(1)	147(1)	243(3)	3(4)
O(4)	16*i*	822(1)	−473(1)	253(4)	3(4)

[a] One-third of the trace of the orthogonal U_{ij} tensor.

Table 3. Main Interatomic Distances (Å), Angles (deg), and the Number of Equal Metal−Oxygen Distances (*n*) for $R_8Ba_5Ni_4O_{21}$ (R = Y and Er)

R	*n*	Y	Er
R1−O2	1	2.419(9)	2.41(3)
R1−O3	2	2.280(6)	2.27(2)
R1−O4	2	2.373(6)	2.38(2)
R1−O3	2	2.367(6)	2.35(2)
R_2−O1	1	2.310(1)	2.300(1)
R_2−O3	2	2.301(6)	2.30(2)
R_2−O4	2	2.321(6)	2.28(2)
R_2−O4	2	2.386(6)	2.37(2)
Ba_1−O3	2	3.115(6)	3.10(2)
Ba_1−O2	2	2.848(1)	2.837(2)
Ba_1−O4	2	2.893(6)	2.87(2)
Ba_1−O2	1	2.685(9)	2.68(3)
Ba_1−O3	2	3.230(6)	3.23(2)
Ba_1−O2	1	2.708(8)	2.71(3)
Ba_2−O4	8	2.904(6)	2.90(2)
Ba_2−O1	2	2.846(1)	2.836(1)
Ni−O3	2	2.010(6)	2.00(2)
Ni−O2	1	2.005(9)	2.01(3)
Ni−O4	2	2.064(6)	2.08(2)
R1−R1		3.663(1)	3.610(1)
R1−R2		3.426(2)	3.385(1)
R2−R2		3.266(2)	3.221(2)
Ni−Ni		4.831(3)	4.758(3)
R1−Ni		2.837(2)	2.820(3)
R2−Ni		3.237(1)	3.201(1)
O3−Ni−O3		87.2(3)	86.8(9)
O3−Ni−O2		107.4(8)	107.6(8)
O3−Ni−O4		89.2(2)	89.2(8)
O3−Ni−O4		158.5(2)	158.6(8)
O2−Ni−O4		94.0(2)	93.7(9)
O4−Ni−O4		86.4(3)	87.0(9)

parameters as well as the main interatomic distances and angles for $R_8Ba_5Ni_4O_{21}$ (R = Y, Er) compounds. The coordination polyhedra for the metals are square NiO_5 pyramids, R atoms that are situated in two different sites and are coordinated to seven oxygen atoms forming trigonal prisms monocapped on one rectangular face; and tetragonal bicapped $Ba(2)O_{10}$ as well as irregular $Ba(1)O_{10}$ polyhedra (Figure 3). The crystal structure can be viewed as formed by columns along the (001) direction. In these crystals, $Ba(2)O_{10}$ alternate with units that are constituted by four $R(2)O_7$ polyhedra that have in common the apical vertex O(1) and thus share triangular faces. This oxygen atom, O(1), is also an apical vertex of the $Ba(2)O_{10}$ polyhedron. Every four of these units, those with equal *z* value, occupy the vertexes of a large square that is the (001) face of the unit cell, and connect with each other in the *xy* plane according to the sequence R(2)−R(1)−Ni−E(1)−R(2): the $R(2)O_7$ polyhedra share edges and $R(1)O_7$ and NiO_5 alternatively have common faces or edges. Every two adjacent cells house pairs of $Ba(1)O_{10}$ polyhedra that share the O2−O2 edge and remain mutually twisted 90° along the *c*-axis. The 3-dimensional structure can also be conceived as the result of stacking infinite $[R_8Ni_4O_{21}]^{\infty}$ layers perpendicular to the *c*-axis. These layers are mutually shifted, obeying the body-centered cell symmetry. The Ba cations are housed in the two kind of different interstices that form between interconsecutive layers (Figure 4). Anisotropic refinements showed that U_{33} thermal parameters are very small in this series of compounds; in some cases they are close

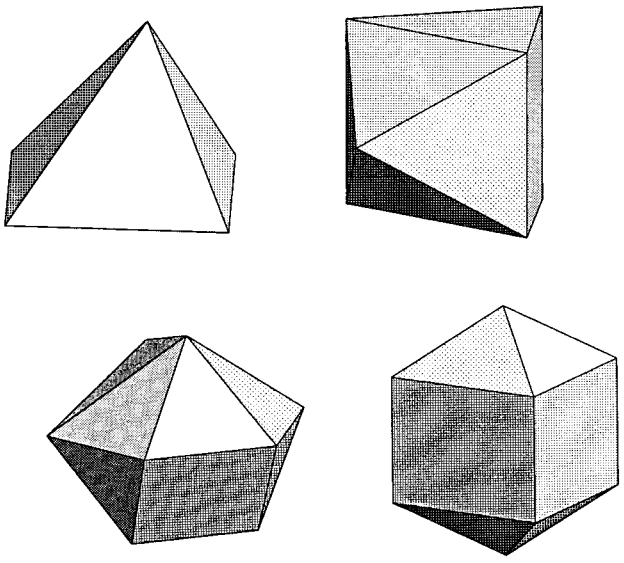

Figure 3. Coordination polyhedra in $R_8Ba_5Ni_4O_{21}$: (top) NiO_5 and RO_7 and (bottom) $Ba(1)O_{10}$ and $Ba(2)O_{10}$.

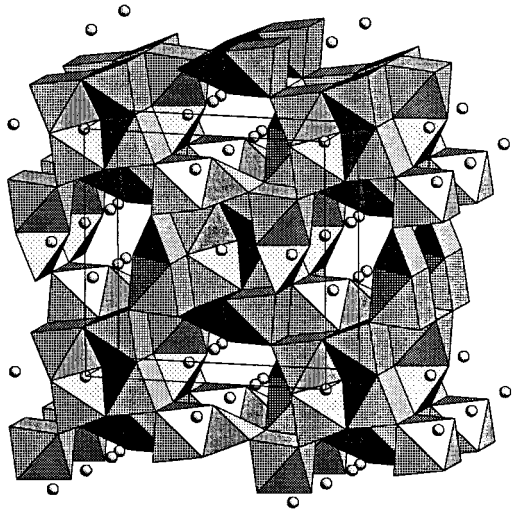

Figure 4. View along *c* direction of the $R_8Ba_5Ni_4O_{21}$ unit cell.

to zero. This smallness could be attributed in part to absorption effects due to the crystal morphology, but also to the existence of some structural anisotropy, given that very compact columns are formed along *c* direction as a consequence of the stacking of the $[R_8Ni_4O_{21}]$ layers.

The crystal structure of the tetragonal $R_8Ba_5Ni_4O_{21}$ = 4 ($R_2Ba_{1.25}NiO_{5.25}$) (I) can be compared with those established for the orthorhombic types, *Immm* for R_2BaNiO_5 (II) and the *Pnma* for R_2BaCuO_5 (III), looking at the coordination polyhedra present in each one. The RO_7 are very similar in the three cases: I and II include two kinds of independent positions for rare-earth atom, with one of the RO_7 polyhedra being slightly smaller than the other. In III, only one independent R atom exists per asymmetric unit. The Ni atom, in the present structural type I is situated in isolated square pyramids that are very similar to those existing in II for the Cu atom. As is known in III, Ni atoms form chains of octahedra by sharing the apical vertex. As with II and III, which include only one kind of Ba polyhedron, BaO_{11} in II and BaO_{10} in III, there are two different Ba atoms in I. Both of the Ba atoms in I are coordinated to 10 oxygen atoms, one of them in a tetragonal bicapped prism that is quite similar to the one found in III and the other one in a very irregular polyhedron whose shape is more like the one in II.

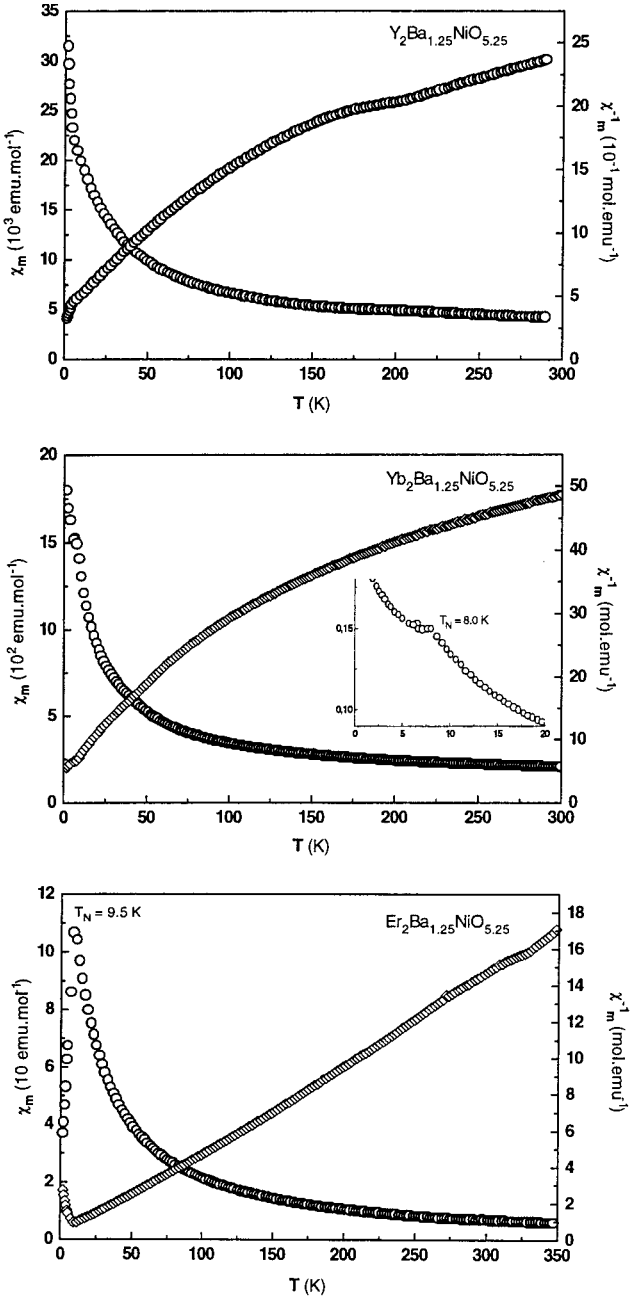

Figure 5. Molar magnetic susceptibility and its reciprocal as a function of temperature for (a) $Y_2Ba_{1.25}NiO_{5.25}$, (b) $Yb_2Ba_{1.25}NiO_{5.25}$, and (c) $Er_2Ba_{1.25}NiO_{5.25}$.

The temperature dependence of the molar magnetic susceptibility χ_m and its reciprocal χ_m^{-1} at 1000 Oe in $R_8Ba_5Ni_4O_{21}$ for R = Y, Yb, and Er is shown in Figure 5. All the calculations have been made per mole of $R_2Ba_{1.25}NiO_{5.25}$. The plots corresponding to the Y and Yb materials present a deviation from linearity over the whole temperature range and do not follow Curie–Weiss behavior. The most clearly observed deviation is that of Y^{3+}, with no *f* electrons, in which even a broad maximum can be seen, like that which occurs in Y_2BaNiO_5.[15–17] Given the vicinity of the two phases in

(16) Martinez-Rodriguez, L. R.; Sáez-Puche, R.; Martinez, J. L.; DeAndres, A.; Taboada, S. *J. Alloys Compd.* **1991**, *225*, 208.

the R−Ba−Ni−O phase diagram, the existence of an impurity of this last compound that is undetectable by X-ray powder diffraction is not ruled out. In the range 25−150 K, the inverse magnetic susceptibility of $Y_2Ba_{1.25}NiO_{5.25}$ follows ($r = 0.998$) the Curie−Weiss law [$\chi_m^{-1} = 55.8(9) + 0.9188(9)T$], with a Weiss temperature of −60.7 K and a molar magnetic moment of 3.0 μ_B. This value agrees with that expected for a paramagnetic five-coordinated nickel(II).

In $Yb_8Ba_5Ni_4O_{21}$, the lack of linearity is more remarkable at temperatures <125 K. At higher temperatures, the susceptibility also obeys the Curie−Weiss law, $\chi_m^{-1} = 23.10(1) + 0.0885(5)T$ ($r = 0.999$), with a Weiss temperature of −260 K and a $\mu_{eff} = 9.64\ \mu_B$, which is about three-fourths the sum of the atomic moments. These data, together with the maximum observed at 8 K in the χ_m plot, indicate an antiferromagnetic ordering of the Yb^{3+} ions at this temperature. Below 100 K, the effect of the crystal-field splitting of the $^2F_{7/2}$ ground state for Yb^{3+} is responsible for the downward deviation from linearity in the χ_m^{-1} versus T plot, as effectively as is observed in other Yb compounds[18,19] in which cooperative magnetic interactions are not present. This effect could be masking, at less in part, the antiferromagnetic signal at 8 K, particularly taking into account its intensity for the $4f^{13}$ configuration of Yb^{3+} and the existence of two independent sites for the rare earth in the asymmetric unit of this structural type.

$Er_8Ba_5Ni_4O_{21}$ is paramagnetic from 15 K. In the range 15−225 K, its inverse magnetic susceptibility follows ($r = 0.9993$) the Curie law, $\chi_m^{-1} = 0.15(2) + 0.0465(1)$ T, with a Weiss temperature of $\theta = -3.3$ K and a molar magnetic moment of $\mu_{eff} = 13.05\ \mu_B$, about one-half of the sum of the atomic moments. The low-temperature data are better illustrated in the χ_m versus T plot. The maximum observed at 9.5 K can be attributed to 3D antiferromagnetic ordering of the Er^{3+} ions. Below this temperature, the susceptibility sharply falls so the magnetic moment at the liquid helium temperature reaches only 4.8 μ_B. This result is unusual and indicates strong interactions that mask the expected crystal-field effect ordinarily present in the mixed oxides at this low temperature.[20]

In the $R_8Ba_5Ni_4O_{21}$ structural type, the Ni−Ni shortest distances are 4.831(3), 4.758(3), and 4.793(4) Å for Y, Er, and Yb, respectively. These are distances between Ni atoms that are at the same *z* coordinate, and along the *z* direction, Ni atoms are situated at distances equal to the *c* parameters 5.6923(8), 5.673(2), and 5.638(2) Å, respectively. Because of the absence of a network of direct Ni−O−Ni superexchange pathway, the interactions will be through a R^{3+}−O−Ni−O−R^{3+} indirect pathway, and thus, the magnetic properties should depend strongly on the type of rare-earth cation R^{3+}. Detailed neutron diffraction investigations are now in progress to determine the magnetic structures.

Acknowledgment. This work was supported by the Spanish DGICYT under Project No. PB94-0031. The authors acknowledge Dr. J. L. Martinez for the magnetic measurements and Dr. C. Cascales for her helpful comments.

Supporting Information Available: Anisotropic temperature factors (1 page) for $Y_8Ba_5Ni_4O_{21}$ and $Er_8Ba_5Ni_4O_{21}$ listings of structure factors (2 pages). Ordering information is given on any current masthead page.

CM980126J

(17) Mompean, F. J.; García-Hernandez, M.; Martinez, J. L.; García-Matres, E.; Prieto, C.; DeAndres, A.; Saéz-Puche, R.; Eccleston Shober, H. *Physic B* **1997,** *234*, 572.

(18) Fernández, F.; Sáez-Puche, R.; Cascales, C.; Marcano, C.; Rasines, I. *J. Phys. Chem. Solids.* **1987**, *48*, 229.

(19) Cascales, C.; Sáez-Puche, R.; Porcher, P. *J. Phys.: Condens. Matter* **1996**, *48*, 229.

(20) Guo, M. D.; Aldred, A. T.; Chan, S. K. *J. Phys. Chem. Solids* **1987**, 48, 229.